Genetic Basis of Rotenone-induced Parkinson's Disease Model in *Drosophila melanogaster*

Honors Thesis

Presented to the College of Arts and Sciences,

Cornell University

in Partial Fulfillment of the Requirements for the

Biological Sciences Honors Program

by

Iyaniwura Olapeju Adunni Olarewaju

May 2020

Dr. Andrew Clark

Abstract

Parkinson's disease (PD) is a neurological disorder that exists in sporadic and familial forms and causes the death of dopamine-producing neurons in humans. Rotenone, a pesticide, can be used to induce a model of sporadic PD in *Drosophila melanogaster.* The genetic pathogenesis of PD is still being determined in both humans and *D. melanogaster*. Conducting a genome-wide association study on the genetic variation of *D. melanogaster* from the Drosophila Genetic Reference Panel (DGRP) with rotenone-induced PD uncovered a set of candidate genes that alter sensitivity to the pesticide. Many of these genes point to possibly important roles of natural variation in the Fibroblast Growth Factor (FGF) Pathway and microtubule synthesis. As microtubule is central to the transport of dopamine in *D. melanogaster*, these findings suggest a possible explanation of sporadic PD in humans based on genetic and environmental interactions.

Background

Parkinson's disease (PD) is a neurodegenerative disorder that is characterized by the loss of dopaminergic neurons. In humans, lack of dopamine results in characteristic motor impairment traits like slowed movements and rigidity. There are two forms of Parkinson's disease: familial, which is caused by inherited genetic mutations, and sporadic, which is often caused by interactions between

genetic and environmental factors (Kieburtz and Wunderle 2013). Sporadic cases are more common, but development is only vaguely understood in both forms.

One of the environmental factors that has been found to be associated with sporadic Parkinson's disease is the pesticide, rotenone (Tanner et al. 2011). Rotenone does not directly stop dopamine production but is known to affect the formation of microtubules (Passmore et al 2017), which are necessary to transport dopamine-filled synaptic vesicles (Yagensky et al. 2016). Dysfunctional or slow microtubule assembly can lead to slow transport of dopamine-filled vesicles, which are prone to leakage, thus increasing the concentration of cytosolic dopamine (Alter et al. 2013). Because dopamine can cause an increase in reactive oxygen species in the cytosol, this can lead to cell death. This has been proposed as a likely mechanism behind extreme sensitivity of dopaminergic neurons to rotenone sensitivity (Dias, Junn, and Maral Mouradian 2014).

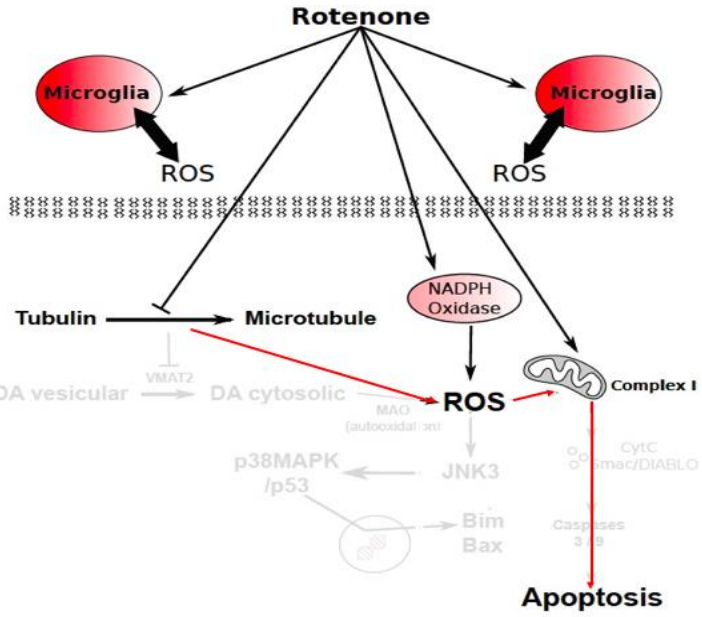

Figure 1: Rotenone leads to cell death. One way it does this is by inhibiting microtubule formation. This contributes to the presence of reactive oxidative species within a neuron, which interact with mitochondrial Complex 1. It also directly interacts with the mitochondrial Complex 1, further accelerating apoptosis. (Adapted from Bisbal and Sanchez 2019)

In *Drosophila melanogaster*, the same pesticide is used to model sporadic PD, as it can recapitulate the phenotypes of Parkinsonian syndrome such as reduced longevity, dopaminergic neurodegeneration and impaired locomotion. The mechanism behind rotenone's effect on PD is not fully understood, but the same tell-tale motor issues seen in rotenone-treated flies are comparable to those seen in humans with the disease, making *D. melanogaster* useful for studying the effects of rotenone on PD (Coulom 2004, Aryal and Lee 2019). *D. melanogaster*

is a good model for Parkinson's disease because 75% of human disease-causing genes have a fly homolog, they breed quickly, and there are many tools to manipulate them genetically and assay their locomotor behaviors in a high-throughput manner (Pandey and Nichols 2011).

D. melanogaster is also a widely used model organism in genotype-phenotype mapping studies thanks to genetic panels such as the Drosophila Genetic Reference Panel (DGRP). This panel consists of 202 inbred lines that were derived from a natural highly polymorphic population (Mackay et al. 2012). All of these lines have sequenced genomes. The DGRP can be used to study the relationship between genotype and phenotype because knowing the DNA sequence of each line provides a way to assess genetic variation as a variable contributing to the phenotype. This is necessary to carry out the genome-wide association studies that highlight the genetic basis of phenotypes such as diseases.

GWAS has been used for the discovery of genetic variants underlying Parkinson's disease in humans. The basic approach is to score the phenotypes and identify the SNPs in genotypes in a large sample of healthy and diseased individuals. The correlation between the variation in phenotypes and genotypes is then used to infer the function of a genetic variant on the expression of a phenotype. Using this approach more than 90 genetic variants have been

implicated in the onset and progression of PD, revealing polygenic genetic architecture of this disease, meaning that many genes influence PD manifestation (Bandres-Ciga et al. 2020). Some of the best characterized genes that carry segregating PD-causing polymorphisms are SNCA, LRRK2, PARKIN and PINK. Interestingly, all four genes have been implicated in microtubule physiology and effect on neurodegeneration (Aryal and Lee 2019), reaffirming the hypothesis that the role of microtubule structure in PD may indeed be significant (Pellegrini et al. 2016).

GWAS using DGRP was used in this study to explore the genetic basis underlying variation in sensitivity to rotenone. By collecting phenotypic data in the DGRP lines from the same fly before and after their exposure to rotenone, we were able to analyze the difference in their climbing abilities, a locomotor phenotype commonly used to score parkinsonian syndrome in flies. Substantial phenotypic variation across genotypes as well as between sexes revealed significant associations of single nucleotide polymorphisms (SNPs) with rotenone resistance. The corresponding candidate genes harboring these SNPs were functionally validated and screened for false positives through rotenone exposure of fly lines genetically modified to have a reduced or no expression of one of the candidate genes. Interestingly, among the candidate genes there were several genes involved in microtubule formation through Fibroblast Growth Factor (FGF) signaling pathway. We propose that polymorphisms in the FGF signaling

pathway may play a role in sporadic Parkinson's disease. To test this hypothesis, we use genetic manipulation (GAL4-UAS system) to downregulate candidate genes in the FGF pathway and test the effect of rotenone on parksinsonian syndrome in flies. We also use the same methods to functionally validate other candidate genes.

Materials and Methods

DGRP fly lines and their handling, rotenone dosing prior to assays

Drosophila Genetic Reference Panel fly lines were ordered from the Bloomington Drosophila Stock Centre. The flies were kept on D food (https://cornellfly.wordpress.com/s-food/) until their exposure to rotenone, for which they were separated by sex. Up to 20 flies were kept per vial, and two vials were set up for each line x sex combination.

To prepare the media, rotenone was dissolved in DMSO and water to achieve 100 μM solution which was then used to hydrate *Drosophila* instant media. The *D. melanogaster* were exposed to this food for 3 days after which they were assayed for startle response.

RING assay and apparatus

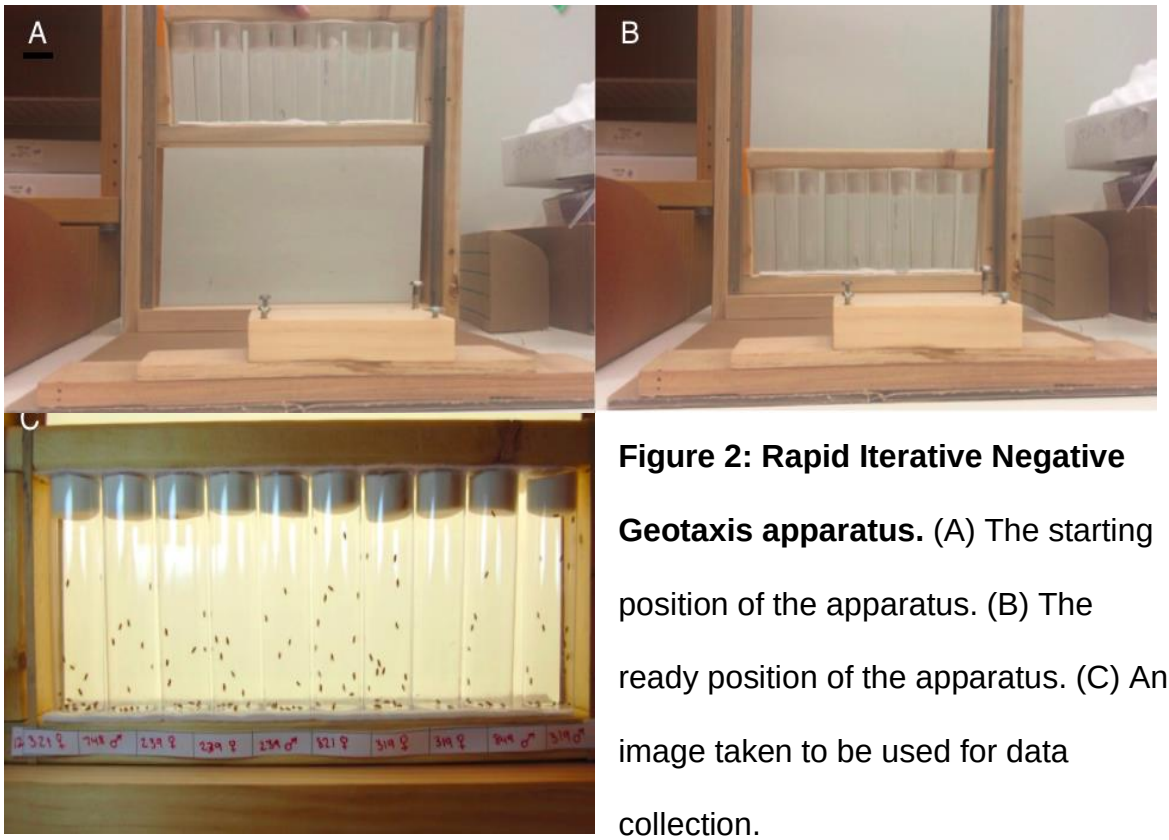

Figure 2: Rapid Iterative Negative Geotaxis apparatus. (A) The starting position of the apparatus. (B) The ready position of the apparatus. (C) An image taken to be used for data collection.

The Rapid Iterative Negative Geotaxis (RING) apparatus resembles a wooden guillotine (Figure 2A, 2B). Two blocks of wood were used to hold 10 vials in place next to each other, with rubber bands wrapped around each end of the blocks (Figure 2C). For the control treatment up to 20 flies were transferred from D-food vials in clean, empty vials, which were arranged to correspond with a strip of paper with the fly line and sex labeled clearly (Figure 2C). After positioning the vials, the wooden block was released and the drop onto the surface of the bench knocked all the flies to the bottom of the vial (Figure 2B). The flies were then given 4 seconds to climb which was recorded by an iPhone timer app. At this

time point, the image of climbing flies was taken by a camera mounted on a stand to ensure that the images were all taken from the same position. This procedure was repeated two times meaning two measurements were taken for each vial. After taking the images, flies were transferred to rotenone fly food media for 3 days after which the RING assay was repeated. In total 115 DGRP lines were assayed and 103 images were taken, resulting in 23,064 climbing height measurements. After the control treatment, all lines were also tested following exposure to rotenone.

Data description and organization

Data was collected from the RING assay images using the software ImageJ. First, each fly in the image was manually labeled using the “multi-point” function, the *x*-*y*-coordinates of the label were recorded, and *y*-coordinates representing the climbed height were exported (Figure 3). Additionally, *y*-coordinates of the bottom of the vial were also recorded so that the climbing height of each fly can be normalized across vials and images (bottom of the vial *y*-coordinate was subtracted from the fly climbing height *y*-coordinate). For each measurement line number, sex, treatment and image label (assaying batch) were recorded.

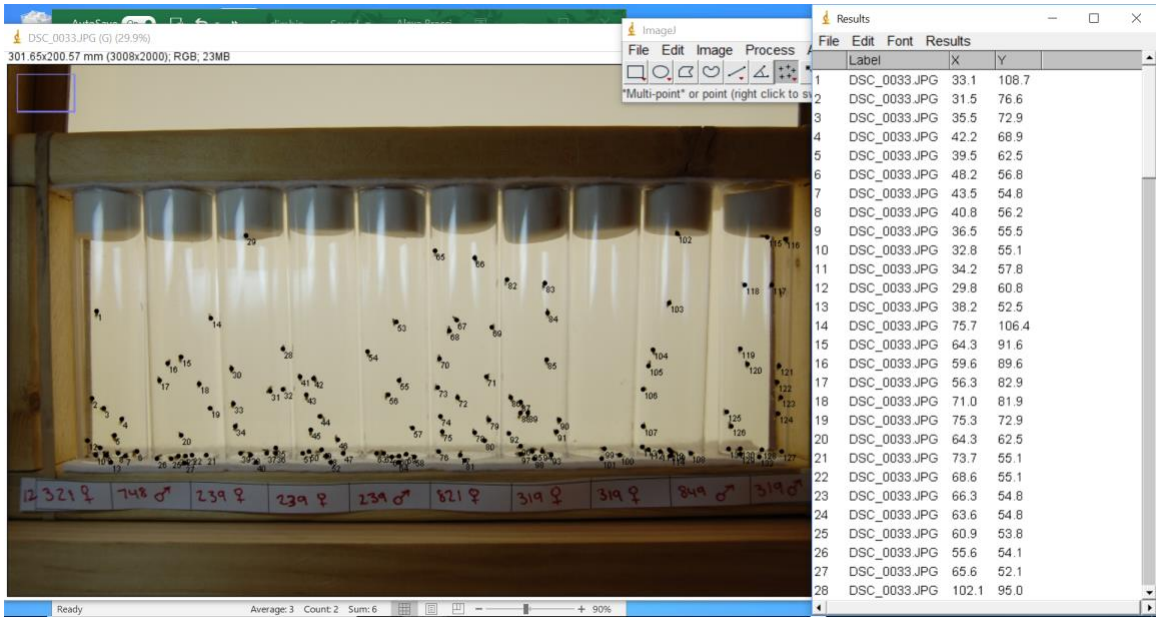

Figure 3: Y-coordinate analysis. Example for an image with individual flies manually labeled as points in an *x*-*y* coordinate system, and automatic recording of *x*- and *y*-coordinates of each point using ImageJ software.

Statistical analysis and genome-wide association

In order to account for the effects of replicate measurements and assaying batch, we fitted a linear mixed model in R to climbing height data using R package lme4 for each of the sexes separately. The effect of batch and replicate measurements were then regressed out and least squared means of line x treatment interaction were obtained using R package lsmeans. Interaction LS means for males and females were supplied to DGRP GWAS software (Mackay et al. 2012) that outputs genotype-phenotype associations for each polymorphic genomic position

in the DGRP. The software also outputs overlap of candidate SNPs with known gene annotations. Where candidate SNPs did not overlap a gene, we manually looked for the closest gene annotation that was downstream of the candidate SNP. To narrow the search pattern, only genes downstream of non-coding variants were considered, however in the future, upstream genes will also be considered.

The GWAS data showed which positions were most significant by sex, so the top nucleotides were narrowed down by function to decipher which were likely to have a role in *D. melanogaster* rotenone resistance.

GAL4-UAS mediated knockdown of gene expression

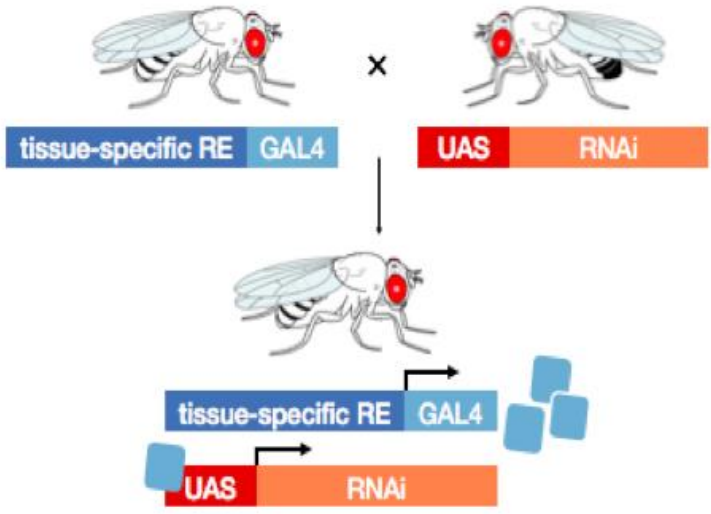

Figure 4: The GAL4/UAS System in *Drosophila melanogaster.* In this illustration, progeny with an active system is created by crossing a female with the GAL4 transcription factor with the UAS enhancer. (Dawn Chen 2018)

To validate the effects of candidate genes yielded by genome-wide association with rotenone resistance, the GAL4/UAS system was used to knock down the expression of these genes and assess whether their expression level plays a role in rotenone-mediated locomotor impairment. The GAL4/UAS system uses the yeast transcription factor GAL4 to drive RNA expression of DNA sequences modified with an upstream UAS enhancer, a specific DNA binding site for the GAL4 protein. Using tissue specific enhancers, the GAL4 protein expression can be contained to specific tissues (Cho et al. 2014). In this study we use GAL4/UAS control of RNAi where we use tissue specific GAL4 drivers to express small interfering RNA that specifically targets transcripts of candidate genes. Using this method we can manipulate the expression of a candidate gene which can help us validate their role in rotenone resistance.

The UAS enhancer can be used to drive expression of RNAi hairpins that use sequence specificity and the siRNA system to downregulate genes (O'Keefe 2020). It can be attached to any DNA sequence. If attached to a piece of artificially designed DNA that forms a short hairpin RNA when transcribed into RNA, this piece of RNA can bind another, complementary piece of RNA like those produced by normal genes. This interferes with the normal gene expression by binding to the gene transcript using sequence similarity and recruiting a complex of proteins that chop down and degrade the gene transcript.

This is RNA interference, or RNAi, which we are using to decrease gene expression. The hairpin RNA is what initiates the degradation process.

By knocking down one gene per line in presence or absence of rotenone treatment before doing the RING assay, we can test the hypothesis that these genes have an effect on rotenone resistance. The resulting data could be understood in one of three ways: after knocking down the gene,

1. the flies could now climb faster, which correlates with the gene increasing susceptibility to rotenone,
2. the flies could climb slower, which correlates with the gene increasing resistance to rotenone,
3. or there could be no significant change in climbing ability, meaning the gene is most likely a false positive and unrelated to the hypothesis in question.

The third outcome is also the null hypothesis.

Candidate gene expression knock down

Three GAL4 drivers were selected based on their tissue specific expression. *elav*-GAL4 drives expression in all neurons, *ple*-GAL4 in the dopamine producing neurons, and *Mef2*-GAL4 in the mushroom body structures. Seeing the effect of gene knock down in all neurons on climbing ability of flies would indicate that a gene is integral to *D. melanogaster* neuronal function. Activity from *ple*-GAL4

suggests that the gene's effect on rotenone resistance is mediated through its expression and function in dopaminergic neurons, which offers a more specific result than *elav*-GAL4 activity. Mushroom body is a neuronal structure downstream of dopaminergic neurons, so if activity is only seen here, this is indicative that the effect of the gene on rotenone resistance is possibly only indirectly dependent on dopaminergic neurons or not at all.

Table 1: GAL4-UAS Crosses.

GAL4 Driver	***elav***	***ple***	***Mef2***
Target tissue / **UAS-RNAi targeted gene**	All	DAN	MBN
AstC-R2			
bnl			
ear			
beat-IIb			
Oamb			
Rdl			
Mipp1			

arm			
sgg			
WDR62			
nAchR2α6			
shep			
Naam			
stai			
htl			

The three GAL4 drivers were chosen because they are expressed in the tissues where we hypothesized the knockdown would have an effect on the climbing ability (all neurons, dopaminergic neurons (DAN) and mushroom body neurons (MBN). The expected effect on climbing ability is indicated by blue color, while lack of effect is indicated by orange color. No color represents no specific expectation for the outcome of the knockdown.

Neurodegeneration assay

To assay dopaminergic neurodegeneration after gene knockdown and/or rotenone treatment, we used a fluorescent protein, Ds-Red, expressed under control of the UAS enhancer and *ple*-GAL driver. This enabled us to visualize dopaminergic neurons at the same time as knocking down expression of candidate genes in the same neurons. After knockdown and rotenone treatment,

adult *D. melanogaster* brains were anesthetized and isolated in a phosphate buffered saline solution in a glass dissection dish under a microscope using tweezers. Any remaining trachea tissue around the brain had to be carefully removed, because their fluorescence would impair scoring of numbers of tagged neurons.

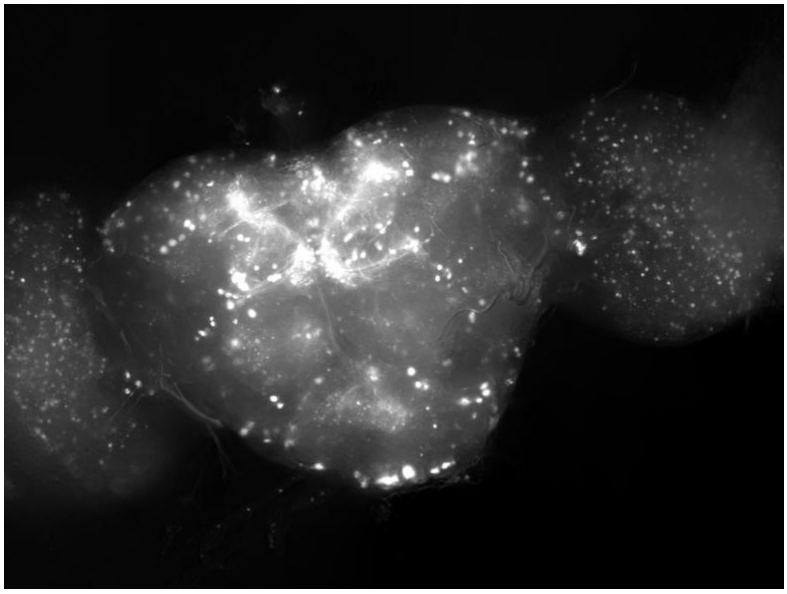

Figure 5: Dopaminergic neurons in adult *Drosophila melanogaster* brain. An example of a maximal projection *z*-stacked image of *D. melanogaster* brain with Ds-Red fluorescence labeling driven by *ple*-GAL4. The use of the *ple* driver resulted in fluorescence in the dopamine-producing neurons, seen in white.

The brains were then mounted (suspended) in PBS on a 384-well plate with flat glass bottom and imaged using a fluorescence microscope. Around 8 to 10 z-plane images are then taken using manual focus and 10x magnification on Echo Revolve microscope in inverted position. Obtained *z*-plane images are then

combined into a focus-stacked maximal projection image of the brain using custom Photoshop script or Zerene stacker software. The *z*-stack was then uploaded to ImageJ which was used to quantify neuron numbers and surface area using Particle count function.

Results

Genome-wide association for rotenone resistance

We tested the rotenone resistance in 120 DGRP lines. Each line was assayed for the difference in their climbing ability with and without rotenone treatment (rotenone sensitivity = control_climbing_height - rotenone_climbing_height). This was done in two replicates of up to 20 flies for each sex. Mean measured control climbing height across all measurements was 26.07 for females and 33.00 for males, while rotenone treated females and males achieved significantly lower heights, 18.99 (t = -17.824, p < 2.2e-16) and 25.70 (t = -15.65, p < 2.2e-16), respectively. Rotenone resistance score was expressed as least square means of the contrast between control and rotenone treatment for each line and sex (where positive values indicate that climbing height is lower for rotenone treated flies than in control flies). The difference in climbing height before and after rotenone treatment ranged between -19.53 and 27.89 for females and -15.52 and 27.57 for males, with a population mean of 7.67 for females and 8.19 for males. Although males and females came from the same batch of flies, their rotenone

resistance correlated only weakly, though significantly (R_2=0.24, *p*-value=0.02) (Figure 6). This result indicates a potentially different genetic mechanism for coping with rotenone toxicity in the two sexes. This prompted us to consider sex-specific genetic effects on this trait. We used an established GWAS pipeline (Mackay et al. 2012) to perform a genome wide association between DGRP genetic variation and their rotenone resistance, taking into account the effects of sex, Wolbachia status and inversion status of each line. There were in total 61 genetic variants that had a significant association with rotenone resistance. Of those, 36, 22, 33 had significant effect on male, female and/or average phenotype, respectively. The effects of 23 variants on rotenone resistance was significant but differed between sexes (Table 2, Figure 7). Many of the significant genetic variants overlapped known gene annotations. Using literature search we looked for previously described functions for genes overlapping candidate variants, focusing on functions related to dopaminergic- or mushroom body neuron functions, as well as functions in mitochondria (Figure 8). This yielded a subset of 13 candidate genes (Table 1) that we chose for further functional validation.

Functional validation of candidate genes

Three of the candidate genes *heartless* (*htl*), *shaggy* (*sgg*), *igloo* (*igl*) play a part in the fibroblast growth factor (FGF) signaling cascade. We were specifically interested in the potential role of this pathway in rotenone resistance. First step in

functional validation was to test if the candidate gene expression is required for rotenone resistance. To test this hypothesis we used GAL4/UAS control of RNA interference to knockdown expression of these genes and measure the effect of rotenone in presence or absence of candidate gene expression. Because FGF signaling can regulate microtubule formation (Figure 9, Gibbs et. al 2017, Callender and Newton 2017) we added additional two genes from this pathway (*stai* and *arm*) to the validation assay using gene knockdown. Parkinsonian syndrome phenotypes such as dopaminergic neurodegeneration and climbing ability after tissue-specific gene knockdown of FGF pathway genes using three different neuronal GAL4 drivers (Table 1) would additionally provide a clue whether this pathway is especially important for dopaminergic neuron function and pathology. These experiments were set up and results were planned to be reported as a part of this thesis. However, SARS-CoV2 pandemic prevented the completion of these experiments before submission of the thesis and were postponed for a later time. However, the expectation for each GAL4/UAS cross is given in Table 1.

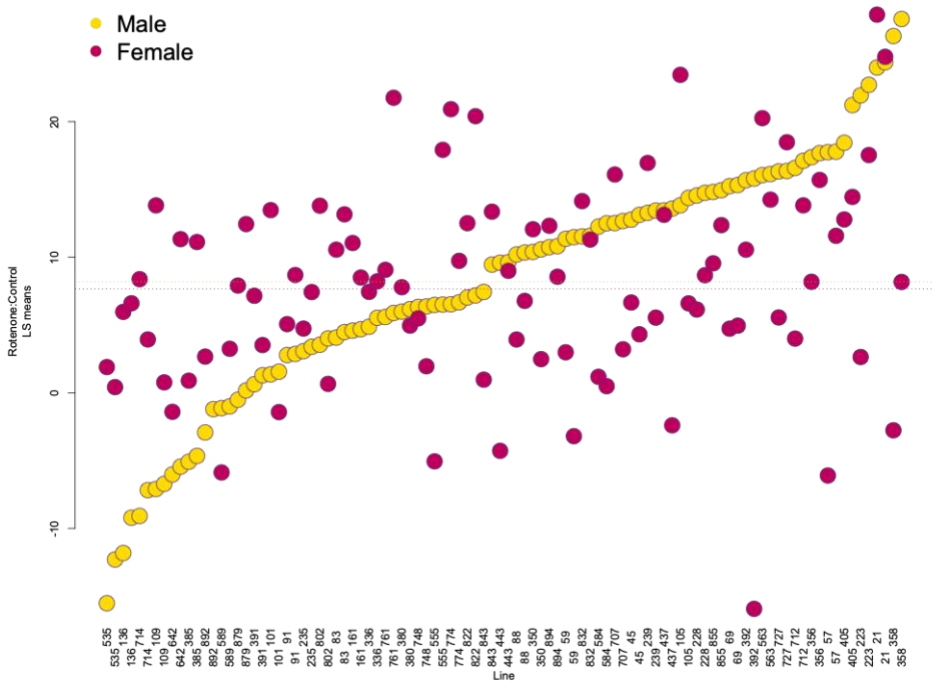

Figure 6: Variation in resistance to rotenone. The Least Squared (LS) means of resistance to rotenone after regressing out the effects of nuisance factors. It can be seen that male and female flies from the same lines do not always follow the same trends in rotenone resistance.

Table 2: Candidate variants associated with rotenone resistance. Red font in gene symbol column indicates closest gene downstream of the variant, while black font indicates overlapping gene. Average *P*-value from mixed effect model is shown. Orange blocks indicate significant association of the variant ($P<10^{-5}$) with rotenone resistance averaged across sexes (A), female- (F) and male-specific (M) effects, and for the different effect between sexes (D).

Variant ID	Minor Allele	Major Allele	ReferenceAllele	Average Effect	Average Mixed Pvalue	FBgn	Gene symbol	Pvalue <10^-5 A F M D
3L_703105_SNP	T	G	G	-4.201	1.18E-07	FBgn0035157	CG13894	
3R_18174862_SNP	T	C	C	-6.06	9.97E-07	FBgn0038946	rdhB	
3L_703115_SNP	A	G	G	-3.715	3.88E-06	FBgn0035157	CG13894	
3L_16565339_SNP	A	G	A	-3.051	4.11E-06	FBgn0026061	Mipp1	
3R_16528612_SNP	C	G	G	-4.462	6.44E-06	FBgn0024944	Oamb	
X_18145143_SNP	T	C	C	-3.638	6.62E-06	FBgn0030904	upd2	
3L_2156426_SNP	A	T	T	3.554	6.68E-06	FBgn0035308	CG15822	
X_5758445_SNP	A	G	G	3.969	6.94E-06	FBgn0262611	CG43137	
X_18146308_SNP	T	A	A	-3.52	8.37E-06	FBgn0030904	upd2	
3R_18172904_SNP	C	A	A	-6.021	9.25E-06	FBgn0038946	rdhB	
2L_1950351_SNP	C	T	T	4.288	1.52E-05	FBgn0031375	erm	
3R_14014755_SNP	C	T	T	3.671	3.98E-05	FBgn0038578	MED17	
3R_18179870_SNP	A	C	C	-5.015	6.72E-05	FBgn0038946	rdhB	
3R_18180441_SNP	A	C	C	-4.987	7.52E-05	FBgn0038946	rdhB	
3R_18177025_SNP	T	C	C	-4.985	7.53E-05	FBgn0038946	rdhB	
3R_18170282_SNP	A	G	G	-4.975	7.72E-05	FBgn0038946	rdhB	
3R_18177049_SNP	A	G	G	-4.957	8.44E-05	FBgn0038946	rdhB	
2R_5646798_SNP	A	C	C	2.837	9.16E-05	FBgn0005614	trpl	
3R_18176717_SNP	G	A	A	-4.926	9.23E-05	FBgn0038946	rdhB	
X_15954532_SNP	C	T	T	4.93	9.24E-05	FBgn0052580	Muc14A	
3R_4341547_SNP	G	C	C	4.228	0.000137	FBgn0037591	Or85C	
3R_24395027_SNP	A	C	C	4.766	0.000163	FBgn0039588	mIF2	
2L_5679830_SNP	T	C	C	-4.43	0.000174	FBgn0031729	CG12511	
2L_5679832_DEL	C	ATATATTCTGCT	ATATATTCTGCT	-4.358	0.000224	FBgn0031729	CG12511	
3L_18493625_SNP	G	A	A	3.313	0.000232	FBgn0036789	AlCR2	
3R_14014818_SNP	T	C	T	2.613	0.000332	FBgn0038578	MED17	
2R_5646811_INS	ACCAACT	A	A	2.64	0.000356	FBgn0005614	trpl	
3R_22282872_SNP	G	T	T	2.397	0.000365	FBgn0039428	CG14237	
2R_5647608_SNP	A	G	G	2.223	0.000501	FBgn0005614	trpl	
2R_5647569_SNP	A	T	T	2.202	0.000528	FBgn0005614	trpl	
X_12509446_INS	A	AA	A	-2.337	0.00076	FBgn0030407	CG2543	
2R_16830480_SNP	T	C	C	4.66	0.000773	FBgn0000044	Act57B	
2R_7951510_SNP	G	A	A	2.738	0.000933	FBgn0033679	CG8888	
3R_13801204_SNP	G	C	C	-2.085	0.001514	FBgn0263995	cpo	
2L_9358433_SNP	A	T	T	-1.992	0.002065	FBgn0085210	CG34181	
X_2561708_SNP	A	G	A	1.961	0.002786	FBgn0003371	sgg	
3L_19663031_SNP	G	C	G	2.427	0.003223	FBgn0036899	tey	
2L_9890436_SNP	G	C	C	3.457	0.003852	FBgn0085212	CG34183	
3L_5423695_SNP	G	T	T	2.199	0.003962	FBgn0085420	CG34391	
3L_5423707_SNP	T	C	C	2.236	0.004969	FBgn0085420	CG34391	
3R_18479497_SNP	G	A	A	3.241	0.006802	FBgn0261572	CG42686	
X_8045337_SNP	T	G	G	2.474	0.015393	FBgn0030011	Gbeta5	
3R_15503124_SNP	T	A	A	2.068	0.016119	FBgn0051216	Naam	
X_8045523_SNP	A	G	G	2.449	0.016558	FBgn0030011	Gbeta5	
X_8045559_SNP	A	G	G	2.374	0.02031	FBgn0030011	Gbeta5	
2L_538277_SNP	A	G	G	-1.756	0.0227	FBgn0003963	ush	
3R_13878850_SNP	T	A	A	3.037	0.031415	FBgn0010389	htl	
X_8044435_DEL	T	TAGCTTAT	TAGCTTAT	2.3	0.056879	FBgn0030010	CG10959	
3R_20606530_SNP	G	C	C	2.647	0.061199	FBgn0259233	CG42331	
3L_17252580_SNP	A	C	C	2.218	0.068598	FBgn0264462	CR43870	
X_8044324_SNP	G	C	C	1.964	0.084155	FBgn0030010	CG10959	
X_8044340_SNP	C	G	G	1.964	0.084155	FBgn0030010	CG10959	
2L_9364405_SNP	T	C	C	1.814	0.111956	FBgn0263323	CG43404	
2L_9364416_SNP	T	C	C	1.814	0.111956	FBgn0263323	CG43404	
2L_9364409_SNP	G	A	A	1.802	0.114426	FBgn0263323	CG43404	
2L_12781230_SNP	A	G	A	0.9968	0.159399	FBgn0032457	CG15483	
3L_6271575_SNP	T	A	A	0.5285	0.534789	FBgn0262787	CG43168	
X_11109608_SNP	G	A	A	-0.2042	0.858664	FBgn0265595	CG44422	
2R_11075854_SNP	C	T	T	0.1165	0.861534	FBgn0013467	igl	
2R_17933057_SNP	A	T	T	-0.2026	0.868059	FBgn0005778	PpD5	
3R_13061509_SNP	A	G	G	0.06121	0.946402	FBgn0038494	beat-IIb	

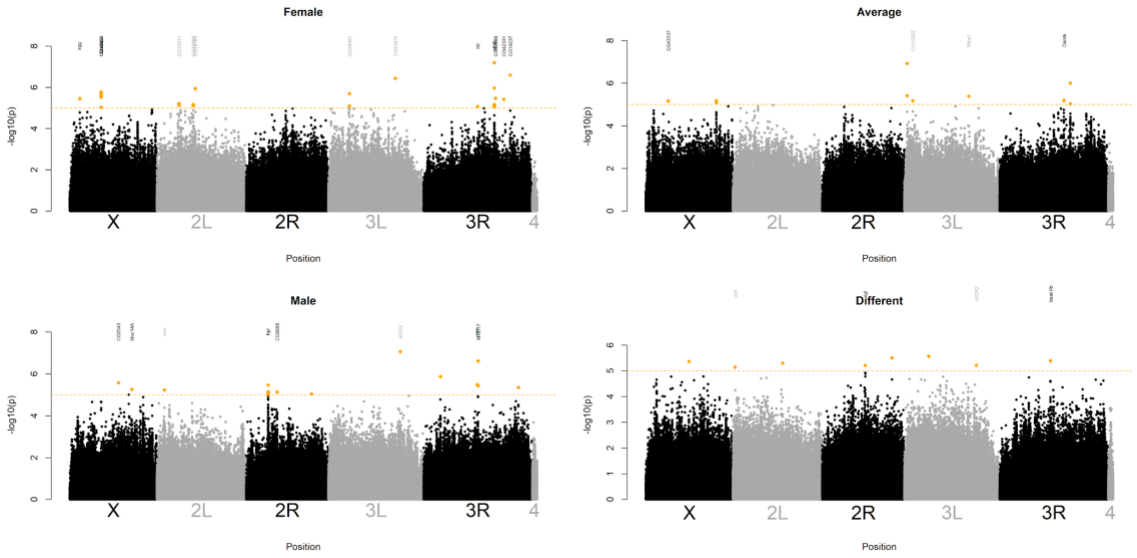

Figure 7: Genome-wide association of genetic polymorphism with rotenone resistance. Manhattan plots for the female- and male-specific associations, associations with the average phenotype, as well as for genetic associations with between-sex differences in rotenone resistance. Variants with significant association with the phenotype ($P<10^{-5}$) are above the orange line and colored orange. Gene names of annotated genes that are overlapping significant genetic variants are also labeled.

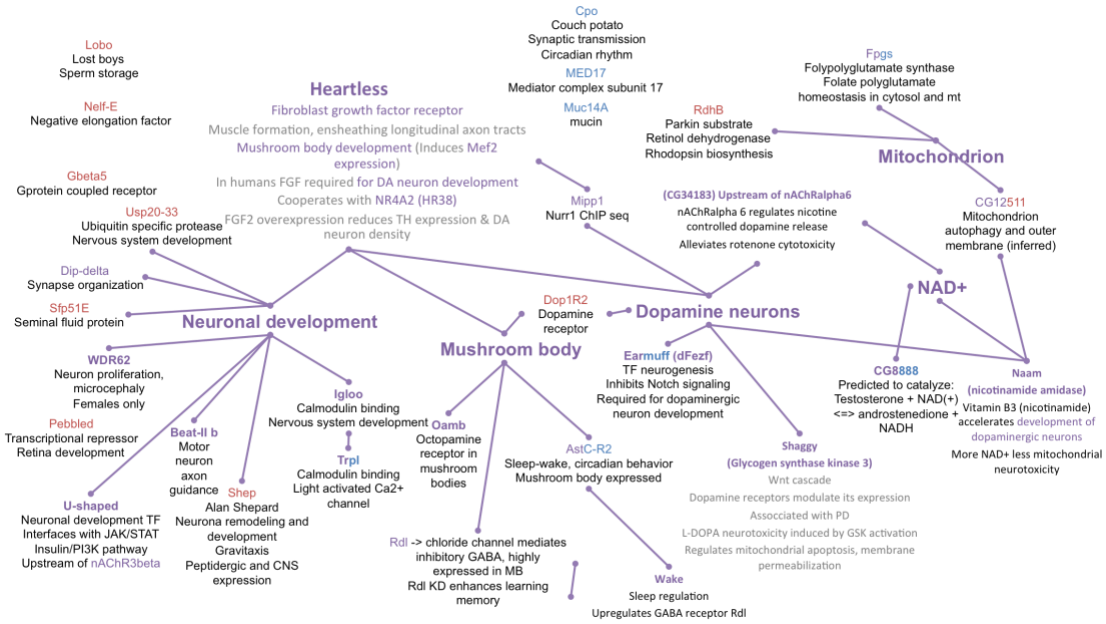

Figure 8: Candidate genes function. Literature search for functions of candidate genes indicated that variation in rotenone sensitivity may stem from variation in genes involved in dopamine- or mushroom body neuron development and function.

Discussion

The objective of this study is to discover candidate genes that modulate the severity of environmentally induced Parkinson's disease. These genes were found by using a Genome-wide Association Study (GWAS) to test for variation in response to rotenone in *Drosophila melanogaster*. We are hypothesizing that the candidate genes nominated through this GWAS screen are involved in rotenone sensitivity.

There are several limitations to this study. First, the GWAS was performed using only 98 lines. The low number of individual genotypes lowers the power to detect significant associations, especially for variants with small effect size. Second, because the GWAS *p*-values have not been adjusted for multiple testing, the candidate SNPs cannot be interpreted as causative but only as suggestive. Subsequent thorough functional validation is necessary to draw conclusions on the effects of the variant candidates on rotenone resistance. Nevertheless, this study provided a list of candidate genomic loci that can be further studied and validated. Interestingly, several of these genes play a role in the fibroblast growth factor (FGF) signaling pathway, which leads to microtubule synthesis, but there are other individual candidate genes. The null hypothesis would be that there is no association between any of these candidate genes and rotenone resistance. Future goals are to test the alternative hypothesis through experimental validation of candidate genes. To do so, we aimed to create genetic constructs for downregulation of the nominated set of candidate genes using a binary GAL4-UAS system available for *D. melanogaster*.

The aim is to express a GAL4 protein in different neuronal tissues which would drive the expression of UAS-RNAi construct in which the RNAi targets the transcripts of candidate genes and at the same time, tag the tissue with DsRed, a fluorescent protein. This will enable us to assay the climbing ability and neurodegeneration of these flies in presence and absence of rotenone while the

candidate gene expression is knocked down. This will provide the first evidence for interaction of rotenone with these genes.

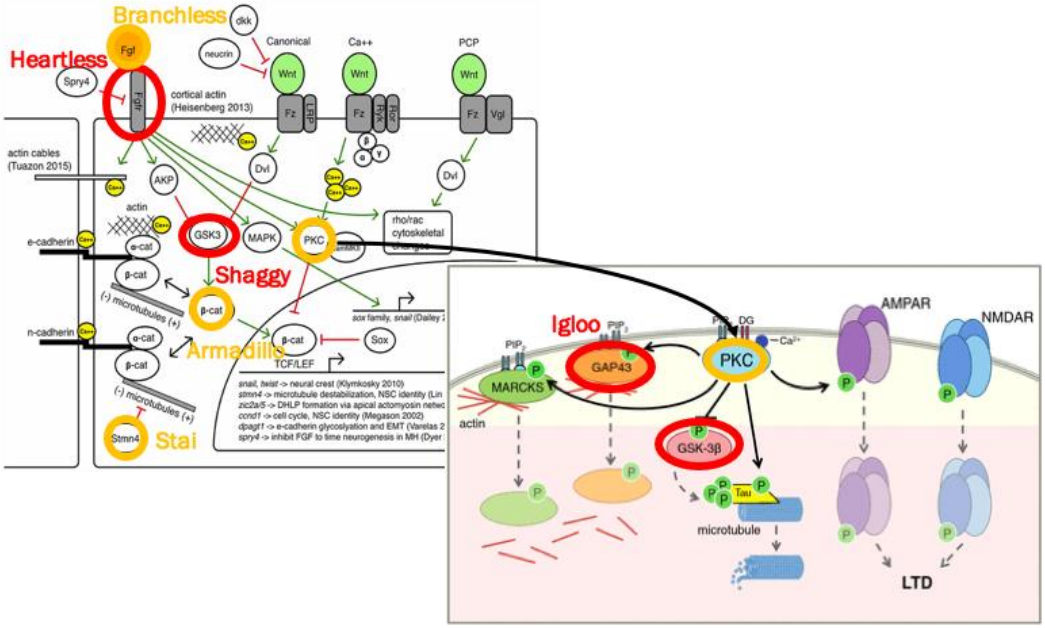

Figure 9: The Fibroblast Growth Factor Pathway. The fibroblast growth factor (FGF) pathway contains many of the genes highlighted by the GWAS, and is also important for the production of microtubule. (Adapted from Gibbs et. al 2017 and Callender and Newton 2017)

The strains will be crossed with the UAS-RNAi construct. That way, we will be able to knock out these flies with a GAL4/UAS system, which allows us to knockout one candidate gene per cross. The protein tagging will allow us to image the *D. melanogaster* brains and determine if the gene knockout affected anything, and where.

The other assay, climbing, will be done before and after the crosses have been exposed to rotenone. The significance in that data will indicate if these genes play any part in rotenone resistance. The driver that we are using, *ple*-GAL4, was chosen because it is expressed in dopamine-producing neurons.

This project will be a confirmation of the validity of our candidate genes. This validation will further the work being done to understand and treat this neurological disease.

Acknowledgements

I have so many people to thank for helping me get to the point of writing a thesis. There are many mentors and peers from the McNair and LSAMP Scholars Programs, who all encouraged me to the very end to commemorate my efforts in lab. Aside from the research, working in the Clark Lab meant a lot of time drinking coffee and watching fireworks on Cayuga Lake, but it also meant that I had the tireless support of Andy Clark and Ana Marija Jaksic to help me go out with my own bang.

References

Alter, S. P., Lenzi, G. M., Bernstein, A. I., & Miller, G. W. (2013). Vesicular integrity in parkinson's disease. *Current Neurology and Neuroscience Reports*, *13*(7), 362. https://doi.org/10.1007/s11910-013-0362-3

Aryal, B., & Lee, Y. (2019). Disease model organism for Parkinson disease: *Drosophila melanogaster*. *BMB Reports*, *52*(4), 250–258. https://doi.org/10.5483/BMBRep.2019.52.4.204

Bandres-Ciga, S., Diez-Fairen, M., Kim, J. J., & Singleton, A. B. (2020). Genetics of Parkinson's disease: An introspection of its journey towards precision medicine. *Neurobiology of Disease*, *137*, 104782. https://doi.org/10.1016/j.nbd.2020.104782

Bisbal, M., & Sanchez, M. (2019). Neurotoxicity of the pesticide rotenone on neuronal polarization: A mechanistic approach. *Neural Regeneration Research*, *14*(5), 762–766. https://doi.org/10.4103/1673-5374.249847

Callender, J. A., & Newton, A. C. (2017). Conventional protein kinase C in the brain: 40 years later. *Neuronal Signaling*, *1*(2). https://doi.org/10.1042/NS20160005

Cho, K. S., Bang, S. M., & Toh, A. (2014). Chapter 26—Lipids and lipid signaling in drosophila models of neurodegenerative diseases. In R. R. Watson & F. De Meester (Eds.), *Omega-3 Fatty Acids in Brain and Neurological Health* (pp. 327–336). Academic Press. https://doi.org/10.1016/B978-0-12-410527-0.00026-0

Dias, V., Junn, E., & Mouradian, M. M. (2013). The role of oxidative stress in Parkinson's disease. *Journal of Parkinson's Disease*, *3*(4), 461–491. https://doi.org/10.3233/JPD-130230

Gibbs, H. C., Chang-Gonzalez, A., Hwang, W., Yeh, A. T., & Lekven, A. C. (2017). Midbrain-hindbrain boundary morphogenesis: At the intersection of *wnt* and *fgf* signaling. *Frontiers in Neuroanatomy*, *11*. https://doi.org/10.3389/fnana.2017.00064

Coulom, H. (2004, December 1). *Chronic exposure to rotenone models sporadic Parkinson's disease in Drosophila melanogaster*. The Journal of Neuroscience : The Official Journal of the Society for Neuroscience. https://doi.org/10.1523/JNEUROSCI.2993-04.2004

Passmore, Jb., Pinho, S., Gomez-Lazaro, M., Schrader, M. (2017, September). *The respiratory chain inhibitor rotenone affects peroxisomal dynamics via its microtubule-destabilising activity*. Histochemistry and Cell Biology. https://doi.org/10.1007/s00418-017-1577-1

Kieburtz, K., & Wunderle, K. B. (2013). Parkinson's disease: Evidence for environmental risk factors. *Movement Disorders*, *28*(1), 8–13. https://doi.org/10.1002/mds.25150

Mackay, T. F. C., Richards, S., Stone, E. A., Barbadilla, A., Ayroles, J. F., Zhu, D., Casillas, S., Han, Y., Magwire, M. M., Cridland, J. M., Richardson, M. F., Anholt, R. R. H., Barrón, M., Bess, C., Blankenburg, K. P., Carbone, M. A., Castellano, D., Chaboub, L., Duncan, L., … Gibbs, R. A. (2012). The drosophila

melanogaster genetic reference panel. *Nature*, *482*(7384), 173–178. https://doi.org/10.1038/nature10811

O'Keefe, E. P. (2020). Sirnas and shrnas: Tools for protein knockdown by gene silencing. *Materials and Methods*. /method/siRNAs-and-shRNAs-Tools-for-Protein-Knockdown-by-Gene-Silencing.html

Pandey, U. B., & Nichols, C. D. (2011). Human disease models in drosophila melanogaster and the role of the fly in therapeutic drug discovery. *Pharmacological Reviews*, *63*(2), 411–436. https://doi.org/10.1124/pr.110.003293

Pellegrini, L., Wetzel, A., Grannó, S., Heaton, G., & Harvey, K. (2017). Back to the tubule: Microtubule dynamics in Parkinson's disease. *Cellular and Molecular Life Sciences*, *74*(3), 409–434. https://doi.org/10.1007/s00018-016-2351-6

Tanner, C. M., Kamel, F., Ross, G. W., Hoppin, J. A., Goldman, S. M., Korell, M., Marras, C., Bhudhikanok, G. S., Kasten, M., Chade, A. R., Comyns, K., Richards, M. B., Meng, C., Priestley, B., Fernandez, H. H., Cambi, F., Umbach, D. M., Blair, A., Sandler, D. P., & Langston, J. W. (2011). Rotenone, paraquat, and Parkinson's disease. *Environmental Health Perspectives*, *119*(6), 866–872. https://doi.org/10.1289/ehp.1002839

Yagensky, O., Kalantary Dehaghi, T., & Chua, J. J. E. (2016). The roles of microtubule-based transport at presynaptic nerve terminals. *Frontiers in Synaptic Neuroscience*, *8*. https://doi.org/10.3389/fnsyn.2016.00003